International Journal of Recent Technology and Engineering (IJRTE)
ISSN: 2277-3878 (Online), Volume-12 Issue-2, July 2023

Misalignment-Related Defect Detection using Discrete Wavelet Transform

Debayan Bhaumik, Debrup Bhaumik

Abstract: *Induction motors are most commonly used in many industries, including petrochemicals, oil, and steel. A single failure in any of the induction motor's components or sub-components can result in a plant shutdown. The plant will suffer significant financial losses as a result. It is crucial to diagnose different types of faults in induction motors. Various condition monitoring techniques diagnose faults in induction motors in the early stages. Vibration analysis is most commonly used among different condition monitoring techniques due to its higher accuracy than other methods. Vibration analysis is used to detect various types of faults in induction motors. The acceleration vibration data corresponding to multiple types of defects are gathered from publicly available web resources. The primary objective of this research work is to explore the severity of horizontal and vertical misalignment defects utilizing a signal processing approach. To achieve this objective, Discrete Wavelet Transform (DWT) is used to detect abnormal behavior of the induction motor. The Daubechies-4(db4) wavelet is chosen as a mother wavelet. As Daubechies wavelet is an orthogonal wavelet, the percentage energy in all decomposed sub-band will equal the original energy of the signal. The energy level of sub-bands is compared with the healthy condition of the motor to detect significant changes in motor fault.*

Keywords: *Induction motor, Vibration analysis, Discrete Wavelet Transform (DWT), Daubechies-4(db4)*

I. INTRODUCTION

Induction Motors are utilized in the power, manufacturing, and transportation industries to transform mechanical power into electrical power. Due to induction motors low cost, adaptability, sturdy construction, appropriate size, and ability to function with any power supply, they have emerged as the industrial world's backbone. The induction motor is made up of three essential parts. The stator, rotor, and bearings are the three components. Induction motor faults occur due to damage to any of its components. Bearing faults are the most common type of fault in an Induction motor. Bearing issues account for 41 to 42% of all defects. Other than bearing faults, stator winding damages range between 28 to 36%. Damages related to the rotor range from 8 to 9%, whereas other types of faults range from 14 to 28%. Bearing and stator winding issues cause the majority of induction motor failures. It's around 69% of total induction motor faults [1].

Vibration analysis is one of the most important ways to recognize different types of faults in induction motors. In this paper, vibration data from accessible sources is collected to distinguish various sorts of faults from healthy conditions on induction motors. The most popular method for locating defects in vibration signals is time and frequency domain analysis. Discrete wavelet transform (DWT) is used to analyse the vibration signal to detect the different types of defects in induction motors. As wavelet transform can work on both time and frequency domains, it can use the signal's time and frequency domain features.

This paper distinguishes horizontal and vertical misalignment defects (mechanical faults) from healthy motor conditions using DWT. The percentage energy of defective conditions is compared with the normal state to detect the defective frequency range for fault analysis of an induction motor.

II. WAVELET TRANSFORM

A wavelet is a form of a small wave. It is concentrated energy in time. It can be used to analyze transient, non-stationary, and aperiodic signals. Wavelet transform (WT) can work on both time and frequency domains simultaneously. WT are classified into two types: continuous wavelet transforms (CWT) and discrete wavelet transform (DWT). The CWT and the DWT differ in discretizing the scaling parameter. The CWT commonly employs exponential scales with bases less than two, like $2^{1/v}$, where v is a positive integer. In general, the scaling parameter in the DWT is discretized to integer powers of 2, such as 2^j, where j is a non-negative integer. CWT is a highly effective approach for determining the damping ratio of oscillating signals. DWT is generally used for denoising, compression, and feature extraction of signals.

The term discrete refers to the discretization of scale and translation parameters. The mathematical expression of DWT follows $s=a_0^m$ and $\tau = nb_0a_0^m$, where s is the scaling parameter and τ is the translation parameter. The DWT of signal $x(t)$ results in coefficients $T(m,n)$ given by (1), where $\Psi_{m,n}(t)$ is the mother wavelet.

Manuscript received on 17 June 2023 | Revised Manuscript received on 22 June 2023 | Manuscript Accepted on 15 July 2023 | Manuscript published on 30 July 2023.
*Correspondence Author(s)
Debayan Bhaumik*, Department of Electrical and Electronics Engineering, National Institute of Technology Karnataka, Surathkal (Karnataka), India. E-mail: debayanbhaumik.212ps008@nitk.edu.in, ORCID ID: 0009-0002-1362-7147
Debrup Bhaumik, Department of Safety Engineering, National Institute of Technology, Rourkela (Odisha), India. E-mail: debrupbhaumik76@gmail.com

$$T\,(m,n) = \int_{-\infty}^{\infty} x(t)\ \Psi_{m,n}^{*}(t)\ dt \qquad (1)$$

$$\Psi_{m,n}(t) = \frac{1}{\sqrt{a_0^m}}\Psi\left(\frac{t-nb_0a_0^m}{a_0^m}\right) \qquad (2)$$

In (1), *'m'* and *'n'* are integers. In (2), 'a_0' and 'b_0' are positive real numbers. In this paper, Daubechies-4 (db4) is chosen as the mother wavelet due to its similar shape with vibrational signals. Daubechies is an orthogonal wavelet. It implies that after decomposing the signal by DWT, the total energy in all detail sub-bands and approximation sub-band will be the same as the original signal [2]. Yumei Kang et al. used the percentage energy of signal using DWT for feature extraction [2]. J. Antonino-Daviu et al. compared the energy of a healthy induction motor signal to broken rotor bar problems to detect induction motor faults [3]. The author also proposed a method for an optimal number of decompositions needed for DWT-based analysis [3]. The total number of decomposition levels required in DWT can be calculated using (3) [3].

$$N = int\left(log_2^{\frac{f_s}{f}}\right) + 2 \qquad (3)$$

An N-level DWT decomposition of a signal results in 'N' detailed sub-bands d_1, d_2, d_3, …., d_N, and one approximation sub-band a_N. This is called the multi-resolution-approximation (MRA) property of DWT. The frequency ranges of the detail sub-band (d_j) and the approximate sub-bands (a_j) are [$f_s/2^{N+1}$, $fs/2^N$] and [0, $f_s/2^{N+1}$] respectively, where fs is the sampling frequency [4].

III. DATA COLLECTION

The data set available online in the public domain is used in this project. MAFAULDA (Machinery Fault Database) vibration dataset is used in this work, which includes vibration data sampled from two 3-axis accelerometers with a 50 kHz frequency [5]. Three operational modes were selected from the open-source data, which are normal sequence, horizontal misalignment defect, and vertical misalignment defect.

A. Normal Sequence

There are 49 defect-free sequences, each with a predetermined rotational speed ranging from 737 to 3686 RPM, with steps of around 60 rpm.

B. Horizontal Misalignment Defect

In this dataset, the motor shaft was moved horizontally by a particular length to create this defect. The diameters of horizontal misalignment defects are 0.5 mm, 1 mm, 1.5 mm, and 2 mm. In the case of horizontal misalignment defects out of 197 datasets, a total of 80 random datasets are chosen for the present analysis.

C. Vertical Misalignment Defect

In this dataset, the motor shaft was shifted vertically by a particular length. The sizes of vertical misalignment defects are 0.51 mm, 0.63 mm, 1.27 mm, 1.40 mm, 1.78 mm, and 1.90 mm. In the case of vertical misalignment defects, out of 301 datasets, a total of 120 random datasets are chosen for detailed analysis.

IV. METHODOLOGY

The horizontal misalignment and vertical misalignment defects of an induction motor will be analyzed with the help of DWT. In order to determine the influence of shaft misalignment in an induction motor, the energy contents of the sub-bands are evaluated. Vertical and horizontal misalignment vibration data from two situations, namely axial and tangential data, are evaluated in this paper.

In this present study, the vibration signals fundamental frequency (f) is 60 Hz, and time-domain samples are obtained with a sampling frequency (fs) of 50 kHz. From (3), it can be deduced that 'N'=11 level decomposition is required to obtain appropriate results. The frequency ranges created by DWT for 11-level decomposition are shown in Table I.

Table- I: Frequency ranges of signals for 11-level decomposition

Decomposed sub-bands	Frequency range (Hz)
d_1	12500.0 - 25000.0
d_2	6250.00 - 12500.0
d_3	3125.00 - 6250.00
d_4	1562.50 - 3125.00
d_5	781.250 - 1562.50
d_6	390.625 - 781.250
d_7	195.312 - 390.625
d_8	97.6560 - 195.312
d_9	48.8280 - 97.6560
d_{10}	24.4140 - 48.8280
d_{11}	12.2070 - 24.4140
a_{11}	0 - 12.2070

Twenty random samples of each defect diameter of horizontal misalignment, vertical misalignment, and normal state of the vibration data of the induction motor are selected and decomposed into 11 levels. The percentage energy of all detail co-efficient levels will be checked and compared with the normal condition of the motor. For calculating the percentage energy of signals, MATLAB has opted.

V. RESULTS AND DISCUSSION

As vibrational signals are non-stationary, the time-frequency domain analysis method can provide accurate results rather than any other signal processing method. In the time-frequency analysis method, DWT is commonly used to determine the severity of misalignment defects due to its better accuracy in detecting mechanical faults. The percentage energies of normal circumstances, as well as different defect diameters, are computed and compared for further analysis.

A. Results related to Horizontal Misalignment Defect (Axial)

The percentage energy in detail sub-band level (d_1 to d_{11}) of 20 random axial data sets of horizontal misalignments of each defect is calculated. The average percentage energy in all detail sub-bands (d_1 to d_{11}) for normal conditions (no misalignment) and axial data of horizontal misalignment defects are shown in Table II.

Retrieval Number: 100.1/ijrte.B78230712223
DOI: 10.35940/ijrte.B7823.0712223
Journal Website: www.ijrte.org

Published By:
Blue Eyes Intelligence Engineering and Sciences Publication (BEIESP)

Table- II: Average percentage energy for normal conditions and horizontal misalignments (axial)

Detail sub-band level	Normal	Horizontal misalignment in mm (axial)			
		0.5	1	1.5	2
d_1	81.97	82.68	82.29	80.42	76.98
d_2	00.50	00.44	00.49	00.45	00.41
d_3	00.47	00.35	00.40	00.41	00.41
d_4	00.54	00.49	00.51	00.56	00.75
d_5	01.03	01.05	01.09	01.20	01.97
d_6	02.65	02.54	02.56	02.74	04.43
d_7	04.17	03.88	04.05	04.67	04.29
d_8	03.68	03.28	03.55	03.92	03.35
d_9	01.69	01.67	01.67	02.16	02.08
d_{10}	01.15	01.16	01.21	01.39	01.35
d_{11}	01.01	01.11	01.07	01.13	01.47

From Table II, it is inferred that the signal energy in sub-band 5 (d_5) seems to increase with the increase in rotor misalignment under horizontal misalignment defect (axial). It shows a definite increasing trend in energy level with increasing misalignment. This is graphically represented and shown in Fig. 1.

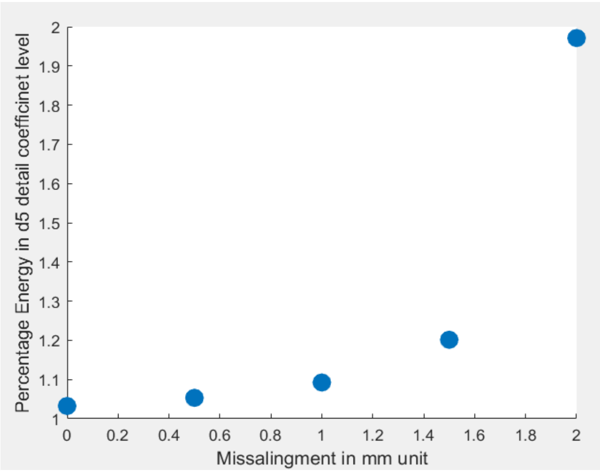

Fig. 1. Trend in percentage energy of sub-band d5 in axial vibration of horizontal misalignment defect.

The percentage change in the energy level of sub-band 5 (d_5) is calculated as given in (4).

$$\%\text{Energy change} = (\text{Energy}_{d5N}-\text{Energy}_{d5ms})/\ \text{Energy}_{d5N} \quad (4)$$

These percentage change in the sub-band energy level of d_5 is tabulated in Table III.

Table- III: Percentage change of energy of d_5 in horizontal misalignment defect (axial vibration)

Horizontal misalignment type of defect (axial)	% Change in detail sub-band 5 (d_5) under defect condition to normal condition
0.5 mm	2.00
1.0 mm	5.80
1.5 mm	16.35
2.0 mm	90.90

B. Results related to Horizontal Misalignment Defect (Tangential)

The percentage energy in detail sub-band level (d_1 to d_{11}) of 20 random tangential data sets of horizontal misalignments of each defect is calculated. The Average percentage energy in all detail sub-bands (d_1 to d_{11}) for normal conditions (no misalignment) and tangential data of horizontal misalignment defects are shown in Table IV.

Table- IV: Average percentage energy for normal conditions and horizontal misalignments (tangential)

Detail sub-band level	Normal	Horizontal misalignment in mm (tangential)			
		0.5	1	1.5	2
d_1	25.53	13.78	09.31	13.52	11.04
d_2	03.59	11.55	13.69	15.53	11.45
d_3	18.78	47.38	51.18	43.25	37.55
d_4	12.78	09.36	08.14	10.52	07.51
d_5	08.82	03.88	04.00	04.54	09.39
d_6	06.00	02.22	03.10	01.84	12.67
d_7	07.94	03.87	04.20	03.16	03.39
d_8	05.35	02.76	02.66	02.56	01.32
d_9	00.88	00.50	00.64	00.33	00.40
d_{10}	03.77	01.46	00.58	01.46	01.19
d_{11}	03.87	01.49	00.90	01.92	01.15

From Table IV, it is inferred that the signal energy in sub-band 8 (d_8) seems to decrease with an increase in rotor misalignment under horizontal misalignment defect (tangential). It demonstrates a clear decreasing trend in energy level as misalignment increases. This is graphically represented and illustrated in Fig. 2.

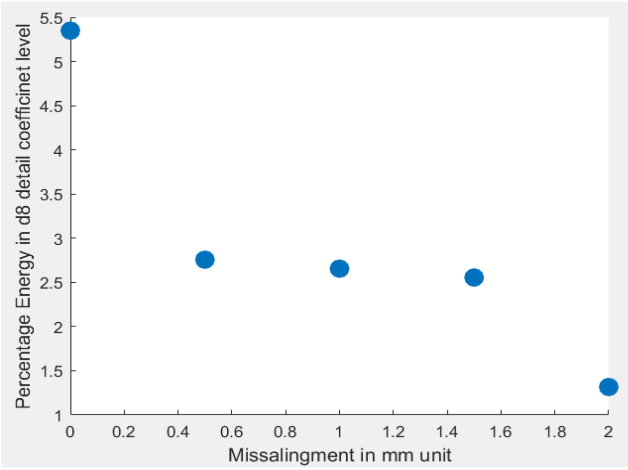

Fig. 2. Trend in percentage energy of sub-band d8 in tangential vibration of horizontal misalignment defect.

The percentage change in the energy level of sub-band 8 (d_8) is calculated as given in (5).

$$\%\ \text{Energy change} = (\text{Energy}_{d8N}-\text{Energy}_{d8ms})/\ \text{Energy}_{d8N} \quad (5)$$

Table V shows the percentage change in the sub-band energy level of d_8.

Table- V: Percentage change of energy of d_8 in horizontal misalignment defect (tangential vibration)

Horizontal misalignment type of defect (tangential)	% Change in detail sub-band 8 (d_8) under defect condition to normal condition
0.5 mm	48.46
1.0 mm	50.35
1.5 mm	52.23
2.0 mm	75.38

C. Results related to Vertical Misalignment Defect (Axial)

The percentage energy in detail sub-band level (d_1 to d_{11}) of 20 random axial data sets of vertical misalignments of each defect is calculated.

Retrieval Number: 100.1/ijrte.B78230712223
DOI: 10.35940/ijrte.B7823.0712223
Journal Website: www.ijrte.org

Published By:
Blue Eyes Intelligence Engineering and Sciences Publication (BEIESP)

The Average percentage energy in all detail sub-bands (d_1 to d_{11}) for normal conditions (no misalignment) and axial data of vertical misalignment defects are shown in Table VI.

Table- VI: Average percentage energy for normal conditions and vertical misalignments (axial)

Detail sub-band level	Normal	Vertical misalignment in mm (axial)					
		0.51	0.63	1.27	1.40	1.78	1.90
d_1	81.9	80.6	81.1	81.14	80.3	78.64	79.18
d_2	00.5	00.4	00.4	00.45	00.4	00.47	00.46
d_3	00.4	00.3	00.3	00.44	00.4	00.48	00.50
d_4	00.5	00.5	00.5	00.74	00.7	00.87	00.95
d_5	01.0	01.1	01.2	01.53	01.7	01.76	01.89
d_6	02.6	03.3	03.2	04.14	04.6	04.75	04.79
d_7	04.1	04.8	04.6	04.02	04.2	04.95	04.38
d_8	03.6	03.0	03.0	03.05	02.7	03.07	02.97
d_9	01.6	02.0	01.9	01.78	01.7	01.76	01.83
d_{10}	01.1	01.3	01.3	00.96	01.0	01.05	01.08
d_{11}	01.0	01.2	01.1	00.78	00.9	00.92	00.92

From Table VI, it is inferred that the signal energy in sub-band 5 (d_5) seems to increase with the increase in rotor misalignment under vertical misalignment defect (axial). It shows a definite increasing trend in energy level with increasing misalignment. This is graphically represented and shown in Fig. 3.

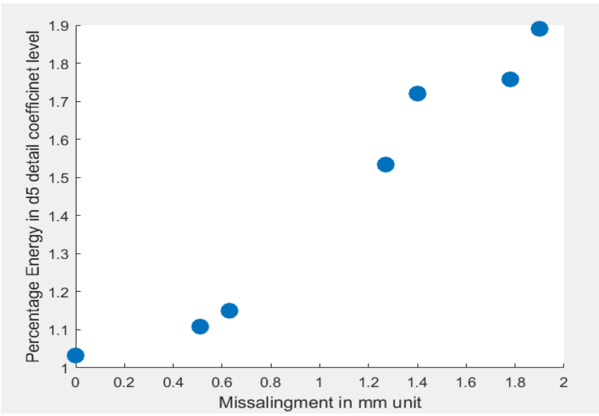

Fig. 3. Trend in percentage energy of sub-band d_5 in axial vibration of vertical misalignment defect.

The percentage change in the energy level of sub-band 5 (d_5) is calculated as given in (6). %Energy change = $(Energy_{d5N}-Energy_{d5ms})/Energy_{d5N}$ (6) These percentage change in the sub-band energy level of d_5 is tabulated in Table VII.

Table- VII: Percentage change of energy of d_5 in vertical misalignment defect (axial vibration)

Vertical misalignment type of defect (axial)	% Change in detail sub-band 5(d_5) under defect condition to normal condition
0.51 mm	07.34
0.63 mm	11.38
1.27 mm	48.55
1.40 mm	66.60
1.78 mm	70.22
1.90 mm	83.08

D. Results related to Vertical Misalignment Defect (Tangential)

The percentage energy in detail sub-band level (d_1 to d_{11}) of 20 random axial data sets of vertical misalignments of each defect is calculated. The Average percentage energy in all detail sub-bands (d_1 to d_{11}) for normal conditions (no misalignment) and tangential data of vertical misalignment defects are shown in Table VIII.

Table- VIII: Average percentage energy for normal conditions and vertical misalignments (tangential)

Detail sub-band level	Normal	Vertical misalignment in mm (tangential)					
		0.51	0.63	1.27	1.40	1.78	1.90
d_1	25.5	13.1	12.8	08.37	07.7	07.43	05.89
d_2	03.5	14.7	14.1	11.88	11.6	11.54	11.12
d_3	18.7	42.4	42.9	44.16	45.5	45.82	45.47
d_4	12.7	07.6	06.9	08.25	08.4	09.22	09.75
d_5	08.8	03.8	04.0	06.01	07.1	06.45	06.77
d_6	06.0	04.5	05.3	09.24	10.5	08.87	08.84
d_7	07.9	05.1	04.9	04.47	03.1	04.52	02.97
d_8	05.3	02.7	02.6	03.13	01.8	03.21	01.84
d_9	00.8	00.3	00.3	00.24	00.2	00.24	00.23
d_{10}	03.7	01.2	01.3	00.80	00.8	00.76	00.73
d_{11}	03.8	01.7	01.5	01.08	00.9	00.96	00.99

From Table VIII, it is inferred that the signal energy in sub-band 1 (d_1) seems to decrease with the increase in rotor misalignment under vertical misalignment defects (tangential). It demonstrates a clear decreasing trend in energy level as misalignment increases. This is graphically represented and illustrated in Fig. 4.

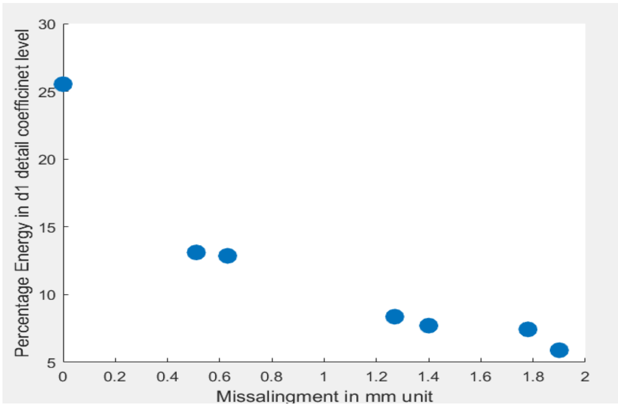

Fig. 4. Trend in percentage energy of sub-band d_1 in tangential vibration of vertical misalignment defect.

The percentage change in the energy level of sub-band 1 (d_1) is calculated as given in (7). %Energy change = $(Energy_{d1N}-EnergyD_{d1ms})/\ Energy_{d1N}$ (7) Table IX shows the percentage change in the sub-band energy level of d_1.

Table- IX: Percentage change of energy of d_1 in vertical misalignment defect (tangential vibration)

Vertical misalignment type of defect (tangential)	% Change in detail sub-band 1(d_1) under defect condition to normal condition
0.51 mm	48.64
0.63 mm	49.63
1.27 mm	67.22
1.40 mm	69.80
1.78 mm	70.88
1.90 mm	76.91

Retrieval Number: 100.1/ijrte.B78230712223
DOI: 10.35940/ijrte.B7823.0712223
Journal Website: www.ijrte.org

Published By:
Blue Eyes Intelligence Engineering and Sciences Publication (BEIESP)

VI. CONCLUSION

The horizontal mismanagement and vertical misalignment defects of an induction motor are successfully discriminated with the help of DWT. Analysis of axial and tangential vibration data using DWT is attempted to identify the influence of misalignment on the decomposition levels of the sub-bands. In the horizontal misalignment defect of the axial data set, the energy content of sub-band d_5 shows a correlation with the degree of misalignment. As misalignment increases, the percentage of energy in d_5 increases. In the horizontal misalignment defect of the tangential data set, the energy content of sub-band d_8 shows a correlation with the degree of misalignment. As misalignment rises, the percentage of energy in d_8 decreases. Hence, the energy content in sub-bands d_5 and d_8 can be used to identify the horizontal misalignment defect. However, the percentage change in energy in the d_5 sub-band is more dominating (by comparing Table III and V). It can be said that the d_5 sub-band frequency range (781.250 Hz to 1562.50 Hz) is responsible for horizontal misalignment defects. In the vertical misalignment defect of the axial data set, the energy content of sub-band d_5 shows a correlation with the degree of misalignment. The energy of d_5 increases as misalignment increases. In the vertical misalignment defect of the tangential data set, the energy content of sub-band d_1 shows a correlation with the degree of misalignment. The energy of d_1 decreases as misalignment increases. Hence, the energy content in sub-bands d_5 and d_1 can be used to identify the vertical misalignment defect. However, the percentage change in energy in the d_5 sub-band is more dominating (by comparing Table VII and IX). It can be said that the d_5 sub-band frequency range is also responsible for vertical misalignment defects. In the case of both defects, sub-band d_5 is responsible for misalignment-related defects. From this, it can be said that wavelet energy in sub-bands can detect various sorts of defects in Induction motors. As vibrational signals are non-stationary, the DWT-based analysis can successfully discern any other induction motor defects with the proper analysis method.

DECLARATION

Funding/ Grants/ Financial Support	No, I did not receive.
Conflicts of Interest/ Competing Interests	No conflicts of interest to the best of our knowledge.
Ethical Approval and Consent to Participate	No, the article does not require ethical approval and consent to participate with evidence.
Availability of Data and Material/ Data Access Statement	The data sets were obtained from the Kaggle community.
Authors Contributions	I, Debayan Bhaumik, completed this research article with the help of Mr. Debrup Bhaumik. This project work can not be completed without the guidance of Mr. Debrup Bhaumik.

REFERENCES

1. Purushottam Gangsar, Rajiv Tiwari, "Signal based condition monitoring techniques for fault detection and diagnosis of induction motors: A state-of-the-art review," Mechanical Systems and Signal Processing, vol. 144, p. 106908, 2020. [CrossRef]
2. Yumei Kang, Hongyuan Liu, Md Maniruzzaman A. Aziz, Khairul Anuar Kassim, "A wavelet transform method for studying the energy distribution characteristics of microseismicities associated rock failure," Journal of Traffic and Transportation Engineering (English Edition), vol. 6, no. 6, pp. 631-646, 2019. [CrossRef]
3. J. Antonino-Daviu, M. Riera-Guasp, J. Roger-Folch, F. Martínez-Giménez, A. Peris, "Application and optimization of the discrete wavelet transform for the detection of broken rotor bars in induction machines," Applied and Computational Harmonic Analysis, vol 21, no 2, pp. 268-279, 2006. [CrossRef]
4. M. Z. Ali, and X. Liang, "Induction Motor Fault Diagnosis Using Discrete Wavelet Transform," 2019 IEEE Canadian Conference of Electrical and Computer Engineering (CCECE), Edmonton, AB, Canada, 2019, pp. 1-4. [CrossRef]
5. "MAFAULDA," Machinery Fault Database [Online]. Available: https://www.kaggle.com/datasets/vuxuancu/mafaulda-full

AUTHORS PROFILE

Debayan Bhaumik, Student, Department of Electrical and Electronics Engineering, NITK Surathkal, India. **About:** Debayan Bhaumik is M.Tech student at National Institute of Technology Karnataka, Surathkal, India. He completed his B.Tech in Electrical Engineering from Jalpaiguri Government Engineering College, India, in 2021. His research interests include condition monitoring of motor faults, machine learning, advanced signal processing algorithms, embedded system, protection, and switchgear.

Debrup Bhaumik, Student, Safety Engineering, NIT Rourkela, India. **About:** Debrup Bhaumik completed his B.Tech in Mechanical Engineering from Brainware Group of Institutions and M.Tech from National Institute of Technology Rourkela. He has expertise in developing effective industrial HSE management systems, providing total safety solutions, mapping safety needs, conducting compliance audits, advising on HSE requirements, and maintaining sound HSE standards as per management system guidelines.

Retrieval Number: 100.1/ijrte.B78230712223
DOI: 10.35940/ijrte.B7823.0712223
Journal Website: www.ijrte.org

Published By:
Blue Eyes Intelligence Engineering and Sciences Publication (BEIESP)